CHAPTER II
LITERATURE REVIEW

2.1 Touchscreen Technology

Tectile or touch sensors devices have been become one of the most importance in any commercially electronic application due to its simplest used and suitable intuitive (Walker, 2012). Touchscreen is an electronic visual display that user can directlycontrol by touching on the screen rather than using a mouse, touchpad or any other controller devices. There was the touchscreen technology used in computers since 1960s (Johnson, 1965). In fact, there were several types of touchscreen technology which used in familiar electronic devices such as automatic teller machine (ATM), stock checking or even cashier computer in convenience store. The reason why using touchscreen technology in these works was using fingers to controller these instruments directly was more convenient than using a keyboard or mouse. About ten years ago, a "personal digital assistant" (PDA), had been the most outstanding electronic instrument which used touchscreen technology. It was controlled by its stylus. However, this technology was still not interested from people enough. Recently, touchscreen technology become highly interesting immediately. According to previous mentioned, the most of current common electronic devices such as smart phones, tablets or even personal computers, all contain touchscreen technology. The unlimited demand and popularity of these electronic devices are driving forces of the touchscreen technology development in the future.

Normally, there are three components used in touchscreen technology: First, "the touch sensor" which is a panel with a touch responsive surface. In generally, touch sensor has an electrical current running through and touching the screen causes a voltage change. The voltage change signals the location of the touching. Second, "the controller" is the hardware that converts the voltage changes on the sensor into signals which computer or other devices can receive. Third, "software" which tells the electronic devices what's happening on the sensor and takes the information coming from the controller. Then, it will allow the electronic devices to respond accordingly.

Walker, (2012) reported that even there were several types of touch sensor, but there have been only four types which were commonly used in general electronic devices. Those are capacitive, resistive, piezoelectric, and multi-component technology.

2.1.1 Capacitive Touchscreen

Capacitive touchscreen or projected capacitive is the most common touchscreen used in many electronic devices. This touchscreen system was invented by Johnson, (1965). The fundamental theory of this type of screen is the electrical voltage disturbing or changing of capacitance of the instrument due to the capacitance of humans's fingers or any conductive objects. Figure 2.1 shows the fundamental theory of capacitive touchscreen works. Conductive layer covered glass at the surface of the screen. At all four corners of the screen generate the electrical voltage to create an electromagnetic field. The electromagnetic field intensity is regular in all area. When humans' fingers touch on the screen, the electrical voltage will decrease. The detector can locate where the point is, then electrical signal will be transformed and sent to the processing unit (Barrett *et al.*, 2010).

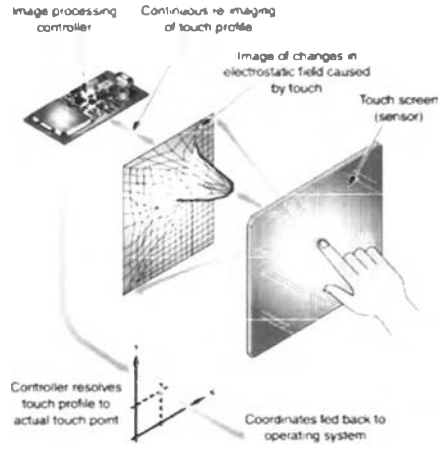

Figure 2.1 The fundamental of capacitive touchscreen.

2.2.2 Resistive Touchscreen

Resistive touchscreen was made by Elo Touch Systems in 1971 (Brown *et al.*, 2007). The original resistive technology was used in and opaque pen digitizer. A resistive touchscreen is simply a mechanical switch mechanism used to locate a touch. The construction of a typical resistive touchscreen is shown in Figure 2.2. A lower layer of glass substrate and an upper layer of flexible film (generally PET) are separated by very small, transparent, insulating spacer dot. One side of both glass and PET are coated with transparent conductive layer of indium tin oxide (ITO). The coated sides are facing each other. The electrical voltage is applied to one or both of the sheets. When a object presses on PET film, the two conductive surfaces make an electrical contact. The resistance between conductive two layers becomes lower, the detector will locate the point and then send the signal to the processing unit as same as capacitive touchscreen technique (Downs, 2005).

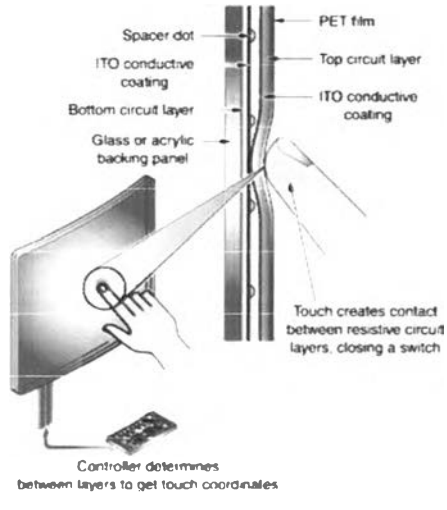

Figure 2.2 The fundamental of resistive touchscreen.

2.1.3 Piezoelectric Touchscreen

Piezoelectric or force-sensing touchscreen is the touchscreen technique which has the fundamental of the piezoelectric property. Piezoelectric materials have demonstrated an ability to convert mechanical energy into electrical energy and vice versa. The electrical signal, generated by stress, may disturb the electro-

magnetic field on the screen. The detector can locate the point and send the signal to the processing unit. Thus this technique can be used as multiple simultaneous touches as capacitive touchscreen (O-Rak, 2013). In advance, the signal generated is directly proportional to the applied force, pressure or strain. So the superior advantage of piezoelectric type over capacitive and resistive type is producing many levels of pressure which can control the intensity of the signal with the pressure-sensor.

2.1.4 Multi-component System

Combining multiple different transducers in one sensor to overcome the shortcomings of each different devices has also been investigated by several researchers. For example, a polyvinylidene fluoride (PVDF) film can acts as pressure sensor, but cannot measure static forces. This limitation can be overcome through the addition of a resistive or capacitive element, and thus making a slip and static force detecting sensor (Dargahi *et al.*, 2006 and Valdastri *et al.*, 2005). Another example, in 2006, Arneson *et al.*, (2006) patented force-sensing touch technology. To make a multi-touch screen with high resolution by combines the advantages of both capacitive and resistive technique. Figure 2.3 shows the diagrams of transparent force sensing layer incorporated in a digital resistive touch screen construction. The fundamental is the same as resistive touchscreen.

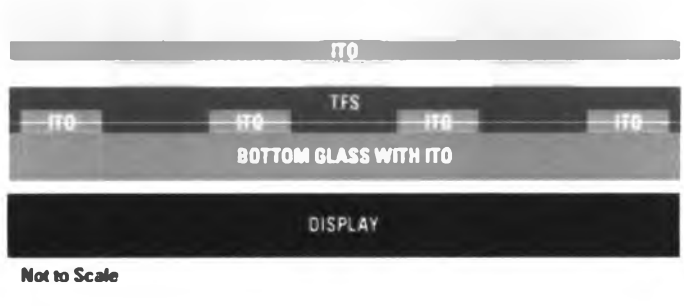

Figure 2.3 Transparent force sensing layer incorporated in a digital resistive touch screen construction.

Due to their difference of fundamental theory, Table 2.1 shows the relative advantages and disadvantages of the touchscreen techniques.

Table 2.1 Touchscreen techniques and their relative advantages and disadvantages

Technique	Modulated parameter	Advantages	Disadvantages	Reference
Capacitive	Change in Capacitance	• Multiple simultaneous touches • Excellent optical performance • Reliable and durable • Excellent sensitivity	• Complexity of measurement electronics • Noise susceptible • Cannot be used with non-conductive objects	• Shashank *et al.*, 2009 • Ko, 2006 • Arshak *et al.*, 2004
Resistive	Changed in resistance	• Cheap • Any objects can be used • High spatial resolution • High scanning rate in mesh	• Cannot use the multiple simultaneous touches • Pressure required • Lower repeatability • Higher energy consumption	• Wen *et al.*, 2008 • Qin *et al.*, 2006
Piezoelectric	Strain (stress) polarization	• High frequency response • High sensitivity • High dynamic range	• Poor spatial resolution	• Qasaimeh *et al.*, 2009 • Li *et al.*, 2008

Technique	Modulated parameter	Advantages	Disadvantages	Reference
Multi-component	Coupling of multiple intrinsic parameters	• Ability to overcome certain limitations via combination of intrinsic parameters	• Discrete assembly • Higher assembly costs	• Dargahi *et al.*, 2006 • Valdastri *et al.*, 2005

2.2 Poly(vinylidene fluoride) (PVDF)

Interest in the electrical properties of PVDF began in 1969 when Kawai, (1969) showed the thin films that had been poled exhibited a very large piezoelectric coefficient, 6-7 pCN^{-1}, a value which is about ten times larger than had been observed in any other polymer as seen in Table 2.2.

Table 2.2 Piezoelectricity in polymer materials (Murayama *et al.*, 1976)

Material	d constant (10^{-13})	Reference
Carnauba wax	-	Adams, 1927
Wax and rosin	-	Meissner and Beckman, 1928
Anthracene {photoelectret}	1.6	Zheludev and Fridkin, 1958
Polymethyl methacrylate	4.3	Kocharyan and Pachadzhyan, 1963
Polyvinyl chloride	13	Kocharyan *et al.*, 1966
Nylon 11	5	Kawai, 1969
Polycarbonate	1	Kawai, 1969
Polyvinyl fluoride	13	Kawai, 1969
Polyvinylidene fluoride	67	Kawai, 1969

The chemical structure of PVDF molecules is given by $(CH_2\text{-}CF_2)_n$. As seen in Figure2.4, PVDF is inherently polar.

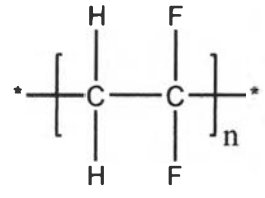

Figure 2.4 Structural formula of PVDF.

The spatially symmetrical disposition of the hydrogen and fluorine atoms along the polymer chain gives rise to unique polarity effects that influence the electrochemical response, solubility, dielectric properties, crystal morphology and yield an unusual high dielectric constant. The dielectric constant of PVDF (not poled) is about 12, which is four times greater than most polymers, and makes PVDF attractive for integration into devices as the signal to noise ratio is less for higher dielectric materials. Other physical properties of PVDF are listed in Table2.3.

Table 2.3 General properties of PVDF piezoelectric film (Murayama *et al.*, 1976)

Property	Unit	Value
Form	-	Metallic film of PVDF
Thickness	μm	9, 15, 30
Size (Tentative)	cm	(MD) 10, (TD) 10
Density	$g.cm^{-3}$	1.78-1.79
Tensile strength	10^7 $N.m^{-2}$	(MD) 25-30
(Yield point)	$kg.mm^{-2}$	(TD) 5-6
Tensile modulus	10^7 $N.m^{-2}$ $kg.mm^{-2}$	(MD) 200-250, (TD) 240-280
Elongation (Yield point)	%	(MD) 18-25, (TD) 4-6

Change in linear dimension at 100 °C, for 30 min	%	(MD) 4-5 {Shrinkage}
Volume resistivity	10^{14} ohm-cm	8-10
Break-down strength	kV {DC} mm^{-1}	150-200
Dielectric constant, 1 kHz		12-13
Dissipation factor, 1 kHz		0.02-0.03

The amorphous phase in PVDF has a glass transition that is well below room temperature (-35 °C), hence the material is quite flexible and readily strained at room temperature. PVDF is typically 50-60% crystalline depending on thermal and processing history and has at least three crystal phases including β-phase,α-phase and γ-phase respectively, which could transform from one to the other under certain conditions. The β-phase belongs to points group C_{2V} with lattice constant, a = 0.858 nm, b = 0.491 nm and c = 0.256 nm; the α-phase belongs to C_{2h} with a = 0.496 nm, b = 0.964 nm and c = 0.462 nm; and the γ-phase belongs to C_2 with a = 0.866 nm, b = 0.493 nm, c = 0.258 nm (Fukada *et al.*, 1981).

The common polymorph of PVDF was α (TG^+TG^-) conformation, which could be produced during crystallization from the melt at atmospheric pressure. One monomer unit for PVDF has a dipole moment of 2.1 Debye. In the α-conformation, successive dipoles make an angle of 120 °C. The average dipole moment for each monomer, therefore, is reduced to 1.05 Debye, but the overall dipole moment in a unit cell is a zero (Fukada *et al.*, 1981). In a unit cell, dipoles for adjacent chains cancel each other. The α-phase crystal is non-polar, non-piezoelectric and non-pyroelectric. The most important polymorph with outstanding piezoelectric properties is β-phase that has a TTTT conformation (all-trans) as show in Figure 2.5. In this β-phase crystal, all dipoles are aligned in the same direction to produce a spontaneous polarization, P_s. A single crystal of β-phase PVDF, if available, should show both piezoelectric and pyroelectricactivites. The γ-phase has a $TTTG^+TTTG^-$ conformation that also exhibits polarizability.

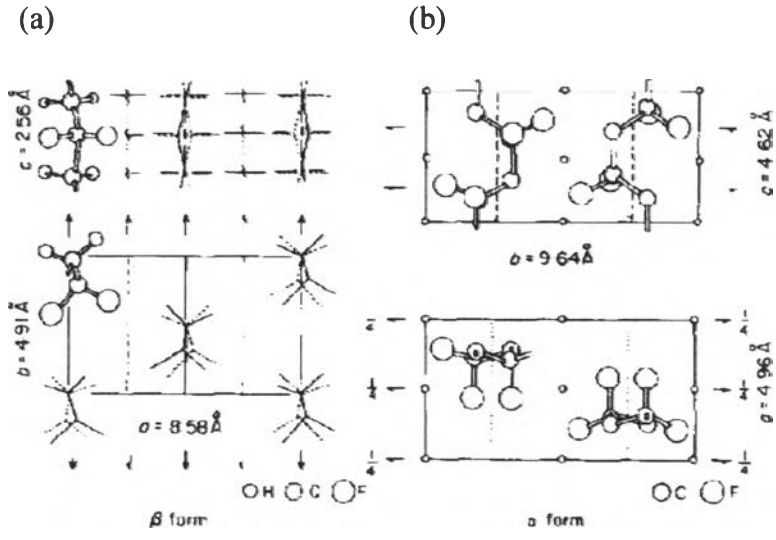

Figure 2.5 Crystal structure of PVDF; (a) β-phase and (b) α-phase (Murayama *et al.*, 1976).

When PVDF is in β-phase structure, the dipole is strongest. This structure aligns all of dipoles throughout the polymer chain creating polarization that extends to the boundaries of the PVDF. These dipoles are allowing PVDF to act as a sensor or transducer. The β-crystal in PVDF could be obtained from a modification by various process such as mechanical deformation, poling under large electric fields, crystallization from the melt under high pressure or very high cooling rates (Nalwa *et al.*, 1995). Different methods for generation of the β-conformation from the melt or from other PVDF conformations are shown in Figure2.6.

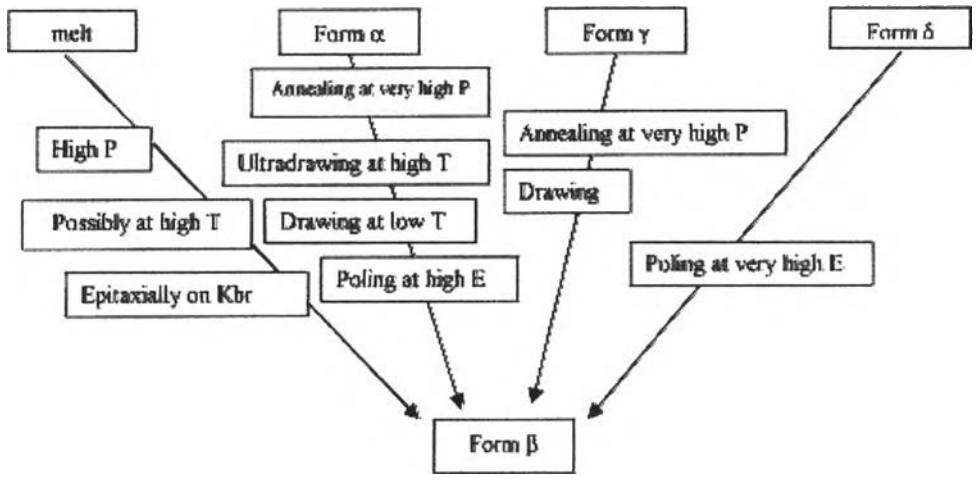

Figure 2.6 Transitions from different conformations of PVDF to β-phase (Nalwa *et al.*, 1995).

2.2.1 Preparation of Piezoelectric PVDF Film

PVDF film can be manufactured by solidification of the film, produced by film-casting extrusion, compression molding, solvent casting and etc.

2.2.1.1 Solvent Casting Method

Lovinger, (1982) developed a very helpful diagram (see Figure 2.7), which indicates the various solvent, such as dimethylformamide (DMF), dimethylacetamide (DMAc), dimethyl sulfoxide (DMSO) and monochlorobenzene (MCB), which along with cyclohexanone are solvents which are used for solvent casting in which the different phase conformational changes and phase transformation mechanisms can be prepared, to produce PVDF films.

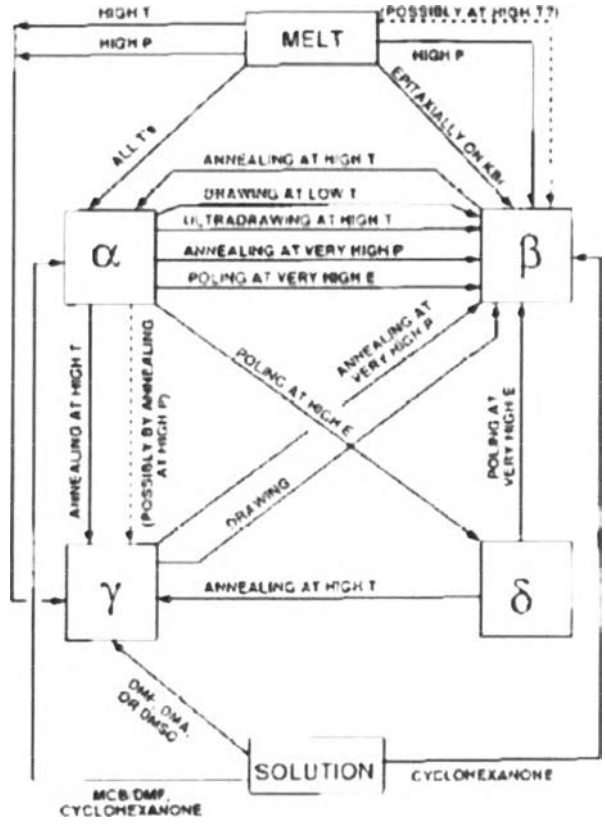

Figure 2.7 The interrelations among the four well-established phase of PVDF (Lovinger *et al.*, 1982).

The variation of solvent polarity and temperature induced a specific conformation in PVDF chains, through the changes in chain coil dimensions and important in stabilizing conformations of PVDF in crystalline phases. Experiments data are shown by Salimi *et al.*, (2004) in Figure 2.8. There was no change on the solution-crystallized films in cyclohexanone (poor solvent) in the temperature range of 50-120 °C. On the other hand, DMAc (good solvent) solution-crystallized films, crystallization mainly results in formation of β-phase at low temperature, whereas at high temperatures α-phase becomes more populated.

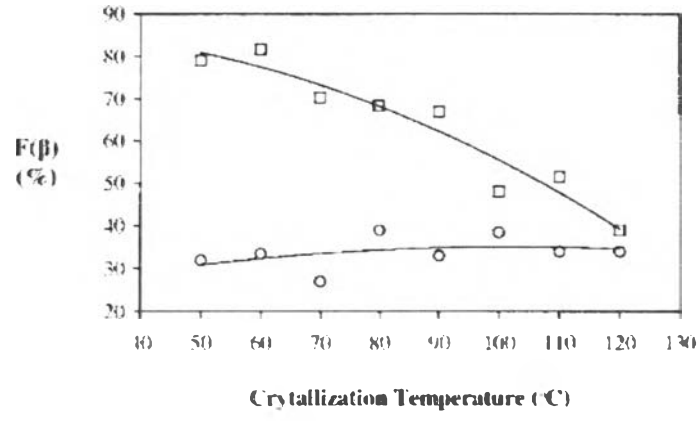

Figure 2.8 Dependence of relative amount of β-phase, F(β) on type of solvent and crystallization temperature for DMAs solution-crystallized (□) and cyclohexanone solution-crystallized (○) (Salimi *et al.*, 2004).

Recently, there's the report from Chinaglia *et al.*, (2009) that's not only crystallization temperature and concentration of PVDF solution have the effect of the amount of β-phase, but solvent evaporation rate has the effect of the amount of β-phase as also. The results were shown in Figure2.9.

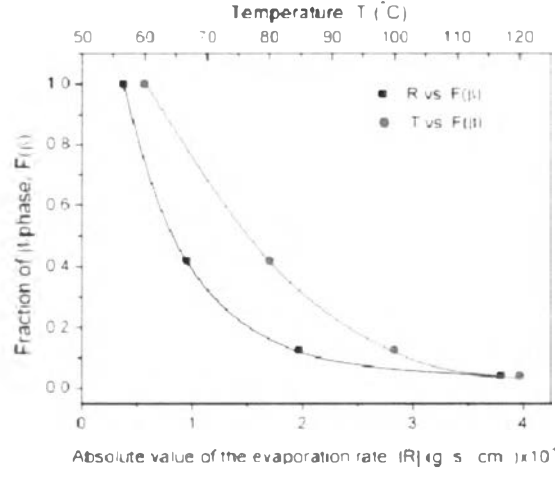

Figure 2.9 Fraction of β-phase, F(β), as a function of the solvent-evaporation rate and the crystallization temperature for initial solution concentrations of 2.5 wt% of PVDF + DMF (Chinaglia *et al.*, 2009).

However, α-phase is thermodynamically more stable in PVDF than β-phase and it is difficult to obtain a β-phase dominant PVDF thin film on a substrate. Applying a mechanical stretching process and poling process in bulk PVDF film can produce transition from α-phase to β-phase.

2.2.1.2 Stretching of PVDF Film

The β-phase can be obtained by mechanism drawing of originally α-phase films as shown in Figure 2.7. Conversion of the α into the β-phase will be efficient when drawing at temperatures lower than 100 °C with draw ratio below 5. Higher temperatures reduced the content of α-phase transformed into β-phase, being above 120 °C practically no conversion occurs, resulting in the oriented α-phase. However, conversion into β-phase can be achieved at higher temperature when draw ratios above 5 (R.P. *et al.*, 2010).

Salimi *et al.*, (2003) studied the effect of stretching on the β-phase in PVDF, the result data was shown in Figure 2.10. It was clearly that β-phase increased with the maximum value at 90 °C with the stretching ratio of 4.5. A maximum value of F(β) was calculated to be 74%. Furthermore, during film stretching, film whitening occurred may be due to stress effects. A necking region and a reduced thickness appeared on the film and propagated along the unstretched portions on both sides during stretching. Necking marked the transformation from spherulitic structure to a micro-fibrillar. Small blocks of lamellar were torn away from the original lamellae to form a fibrillar structure of crystallites. This mechanism induced β-phase structure in PVDF film.

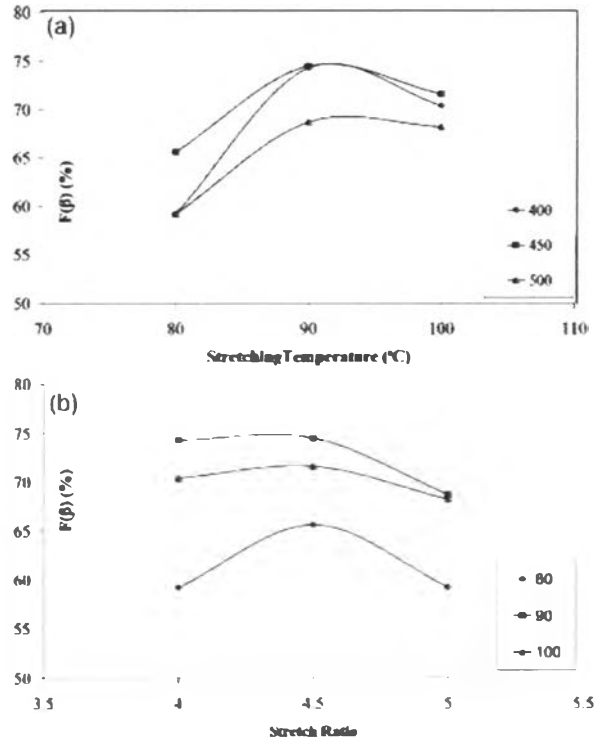

Figure 2.10 Variation of β-phase content for Kynar 720 as a function of (a) stretching temperature and (b) stretch ratio (S.R. = $\frac{Length_{final}}{Length_{initial}}$) (Salimi *et al.*, 2003).

Oriented β-phase films were obtained by utilizing two different techniques; by uniaxial stretching at 80 °C of completely α-phase films (from melt processing at 230 °C), and by uniaxial drawing at 90 °C almost β-phase films obtained by crystallization at 60 °C from DMF solution casting with subsequent pressing at 140 °C (Branciforti *et al.*, 2007). The PVDF films from solution casting had a cloudy appearance and low toughness due to the porosities that occurred from solvent evaporating. To reduce these porosities, uniaxial pressing at 15 MPa and 140 °C for 10 min was applied. This procedure did not affect the PVDF crystalline phase due to the crystalline melting temperature of PVDF was above 160 °C. At this temperature, films would become more transparent and less porosities.

Table 2.4 Crystallinity degree from DSC techniques, F(α) and F(β) (Branciforti *et al.*, 2007)

Sample	X_c (%)	$f_{\alpha,DD}$	$f_{\beta,DD}$
A80R2	-	0.351	0.615
A80R3	42.5	0.382	0.632
A80R4	41.3	0.427	0.658
A80R5	40.6	0.432	0.689
B90R3	49.8	-	0.842
B90R4	45.4	-	0.885
B90R5	45.4	-	0.886

From Table 2.4, Brancifortie*t al.*, (2007) found that increasing the stretching ratio would decrease the degree of crystallinity, this indicated that stretching would destroy the crystalline structure, but increased the α and β-phase crystal. However, the β-phase films still had very high F(β) (88.5%) and moderate amount of crystallinity (45.4%).

Also as Chang *et al.*, (2008) who studied the effect of stretching on thermomechanical and optical characteristics of PVDF by investigated these characteristics at different stretching ratios and different temperature. They found that the fraction of the β-phase was almost saturated for stretching ratios above four. In addition, PVDF films easily cracked and broke formation when they were stretched at the ratios more than 6. Furthermore, thickness of films would be decreasing with the increasing of stretching ratios as shown in Figure2.11. For optical characteristics, they indicated that PVDF films were stretched over three times of their original length at temperature above 80 °C would have transmittance of higher than 80% in the range of visible light as shown in the Figure 2.12 and 2.13.

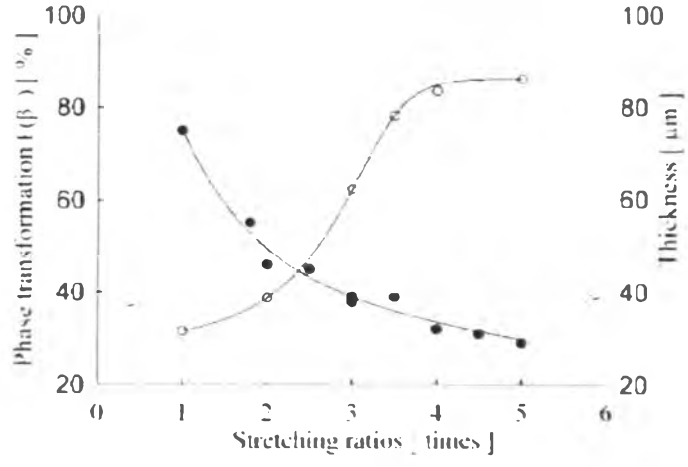

Figure 2.11 The F(β) fraction content and thickness variation of PVDF films with different stretching ratios (Chang *et al.*, 2008).

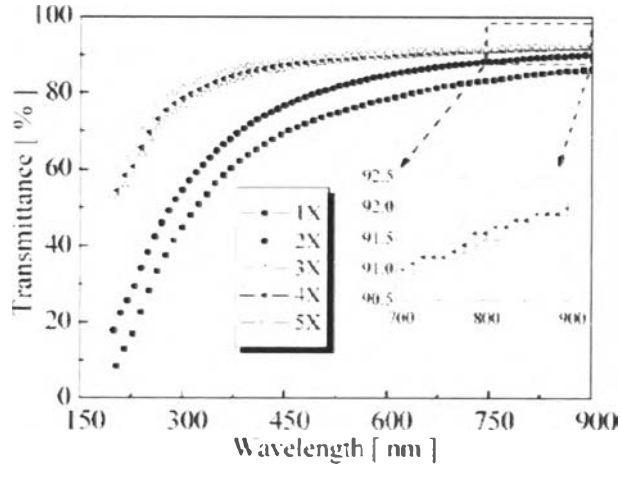

Figure 2.12 PVDF films in UV light with the variation of stretching ratios at the temperature of 80 °C (Chang *et al.*, (2008).

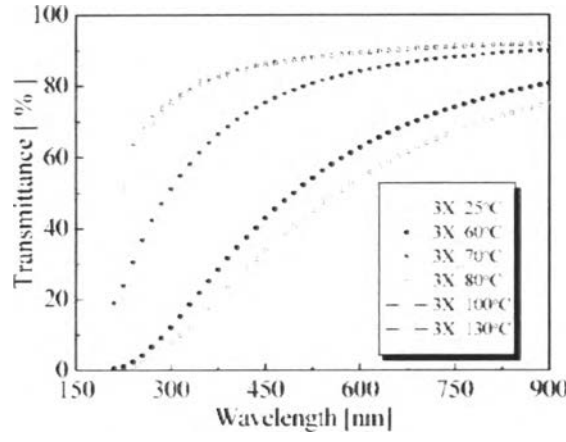

Figure 2.13 PVDF films with a stretching ratio of 3 at different temperatures (Chang *et al.*, 2008).

Miranda *et al.*, (2008) determined that the α to β-phase transformation in silver nanoparticles doped PVDF nanocomposites. The maximum β-phase PVDF was achieve at 80 °C and a stretching ratio of 5 as shown in the Figure2.14. However, from Figure2.15, SEM analysis revealed that the spherulitic structure was destroyed changing into a new structure formed by microfibrils aligned in the drawing direction and proved that the inclusion of nanoparticles has no relevant effect in the microstructure of the polymer.

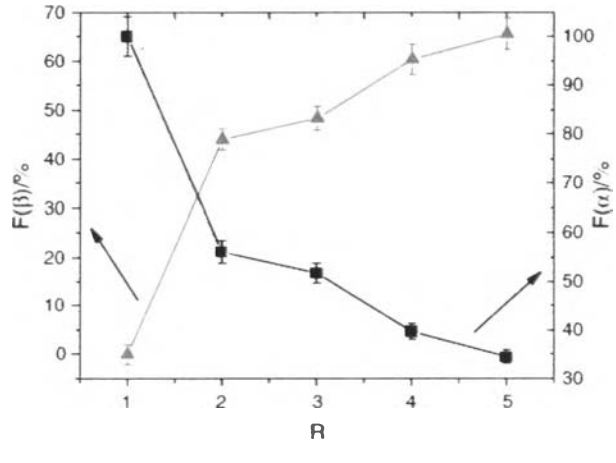

Figure 2.14 Evolution of α to β-phase transformation for 0.012%Ag samples. Sample were stretched at 80 °C (Miranda *et al.*, 2008).

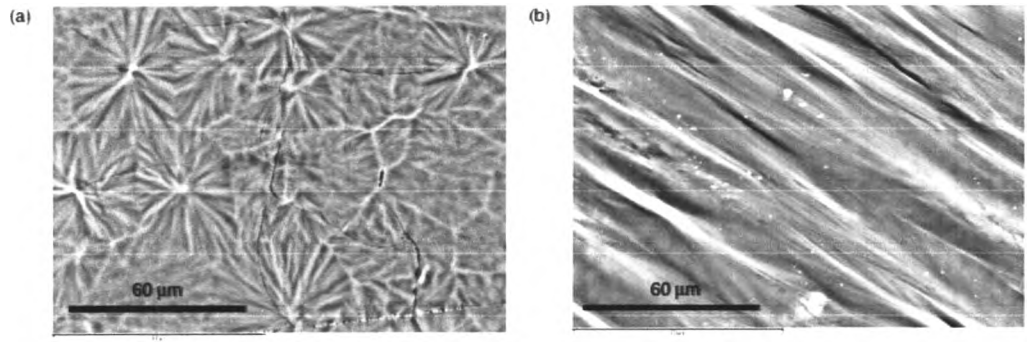

Figure 2.15 SEM images of the PVDF/Ag nanocomposites with: (a) R=1 and (b) R=5 (Miranda *et al.*, 2008).

Moreover, even if the presence of Ag nanoparticles was expected to promote a clear change in the UV-visible spectrum of the nanocomposites and that's make the PVDF films become color, but at R = 5, the surface plasmon resonance (SPR) band can't be distinguished any more due to the local decrease of Ag effective concentration since during drawing the silver nanoparticles are torn away from each other, therefore decreasing the local concentration and diminishing the relative SPR effect, affected the PVDF films become colorless.

Although β-phase was occurred in PVDF film, the dipole moments of PVDF film are randomly oriented resulted in no net dipole. Also the highest piezoelectricity was obtained from certain poling conditions.

2.2.1.3 Poling of PVDF Film

Unpolarized semi-crystalline polymer such as PVDF do not usually make large piezoelectric coefficient because the piezoelectric effect originates from induced polarization andtheir dipole moment is not aligned. To induce polarization, so the dipoles in PVDF film must be reoriented through the application of a strong electric field at elevated temperature. The temperature is then lowered in the presence of the electric field so that the domains are locked in the polarized state. The material's piezoelectric effect is directly related to the degree of polarization achieved. Due to polymers typically possess a high dielectric breakdown and high operating field strength (see Table 2.2), so they can withstand much higher electric

field input than ceramics. The two most common techniques to induce polarization in piezoelectric polymers are electrode and corona poling (Dargaville *et al.*, 2005).

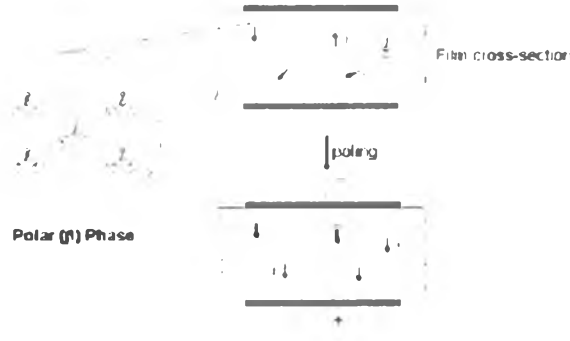

Figure 2.16 Reorientation of the β-phase dipoles in PVDF via poling (Dargaville *et al.*, 2005).

Ramos *et al.*, (2005) reported that poling had two main effects at a structural level, the reorientation of the dipoles along the field direction and the transformation from the α-phase to β-phase, the Figure 2.17, show the decreasing of the absorbance of the 763 cm^{-1}due to the α to β transformation occur by the poling process.

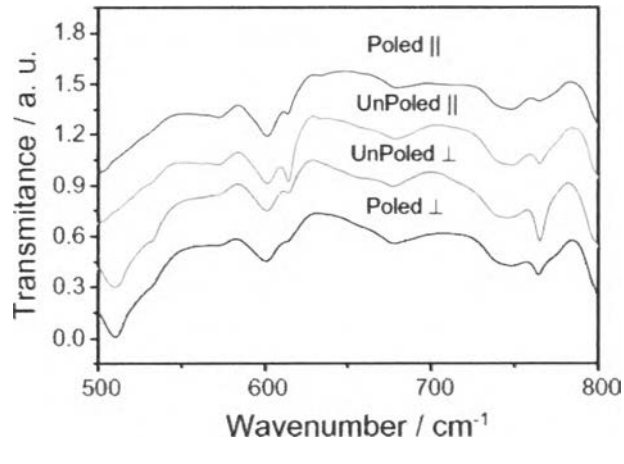

Figure 2.17 FT-IR spectra of poled and non-poled samples of β-PVDF 500 cm^{-1} to 800 cm^{-1} region. (Ramos *et al.*, 2005).

Huan *et al.*, (2007) studied the influence of poling on the structural and piezoelectric properties of Poly(vinylidene fluoride-hexafluoropropylene), (PVDF-HFP) copolymer films, they found that poling process had greatly effect on piezoelectric coefficient d_{33} as shown in the Figure 2.18 due to higher β-phase content even similar amount of crystallinity.

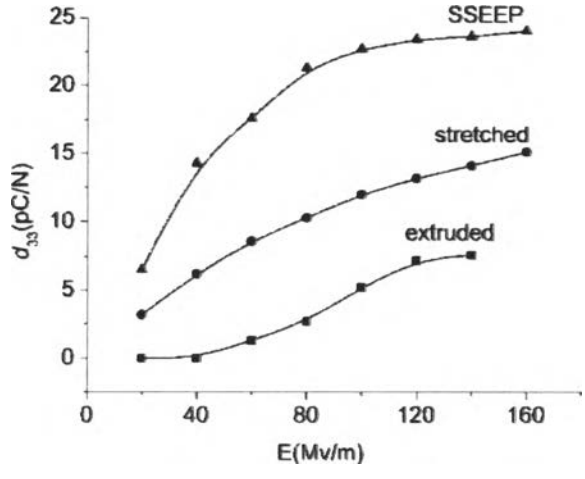

Figure 2.18 Poling field dependence of piezoelectric coefficient d_{33} for extruded, stretched and static electric field poling (SSSEP) (Huan *et al.*, 2007).

There's a report from Jiang *et al.*, (2007), they studied the effect of thermally poled (process : voltage is 5 kV, temperature is 90 °C, and time is 60 min) and corona charged (process : voltage of needle electrode 25 kV, voltage of mesh grid electrode = 5 kV, temperature = 60 °C, time = 1 min) on PVDF films. It was found that both polarized methods contributed to dramatic improvement on the piezoelectricity and ferroelectricity of PVDF films, while thermal poling leaded to structure change with the generation of new carbon composition due to defluorinated from PVDF main chain under strong influence such as heat, electricity. This could be proved in the Table 2.5, that showed the presence of C=C bond on the surface of sample by XPS.

Table 2.5 Elemental composition and binding energies of untreated and polarizing PVDF characterized by XPS (Jiang *et al.*, (2007)

	Carbon (Cls)				**Fluorine (Fls)**
Surface	C=C (eV)	C-C (eV)	C-H,C-H_2 (eV)	C-F_2 (eV)	F-C, F-C-F (eV)
Untreat	-	284.778	286.200	290.619	690.441
Thermal	281.622	284.729	286.436	291.087	690.290
Corona	-	284.610	286.110	290.162	690.222

Moreover, they also reported that the corona charging method yielded a high degree of β-fraction in crystalline and degree of crystalline dipole alignment from calculating the Gergorio equation by using absorption intensity of β-phase and α-phase that obtained by FT-IR spectra (F(β) = 67% and 60% for corona charging and thermally poling respectively) and degree of crystalline dipole alignment from higher remnant polarization (7.5 $\mu C/cm^2$) compared with thermally poled samples (6.3 $\mu C/cm^2$). The more orientation and alignment of dipoles under corona charging conditions could be described by the scission reaction took place due to higher poling electric field and this caused the increasing in molecular mobility and induced polymer molecules from the amorphous region to crystalline or other crystalline phases to polar β-phase crystalline.From all the results, it was concluded that corona charging treatment caused no detectable change in polymeric structure but improved the P_r of PVDF than those treated by thermally poling.

Long term piezoelectricity behavior by using thermal poling and corona poling were compared by Betz, (1984), he found that the decrease of d_{33} with time for the thermally poled samples was in the order of 25 percent within the first months, as the decrease in corona charged samples was limited to 8 percent, the results were shown in the Figure 2.19 and 2.20. The piezoelectricity of PVDF film remains constant for many years, if it is not influenced by the effect of moisture uptake or elevated temperature.

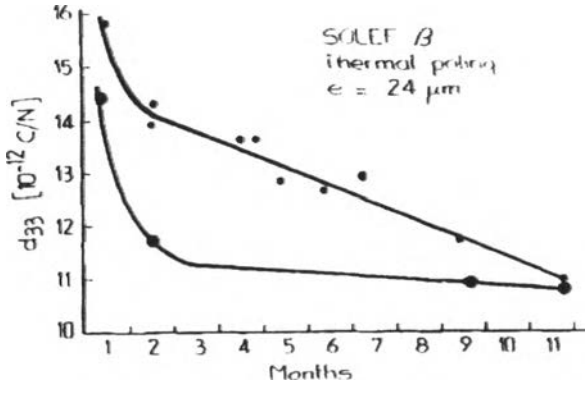

Figure 2.19 Long term behavior after thermal poling (Betz, 1984).

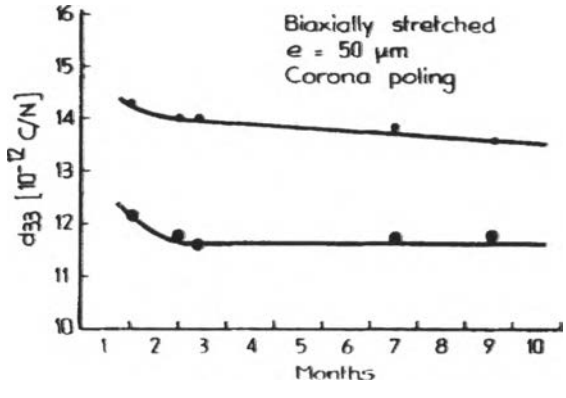

Figure 2.20 Long term behavior after corona poling (Betz, 1984).

From the experiment by Salimi *et al.*, (2004),they indicated that before poling, all films even stretching showed a zero piezoelectric coefficient as shown in Table , whereas after poling under a constant corona field of 1.25 MV/cm, all films exhibited quite high piezoelectric coefficient. These results showed that although formation of β-phase is of the vital importance in piezoelectric applications, it did not affect considerably the piezoelectric coefficients due to the dipole moment in the crystalline part might not align and this randomly oriented resulted in no net dipole, thus a zero piezoelectric coefficient was observed.

Table 2.6 Comparative data of F(β) and stress piezoelectric constant (d_{33}). Before and after stretching the PVDF films. All films samples were exposed under the constant corona field of 1.25 MV/cm (Salimi *et al.*, 2004).

Film drying temperature (°C)	**Unstretched**		**Stretched**	
	F(β) (%)	d_{33} (pC/N)	F(β) (%)	d_{33} (pC/N)
60	82	0	82	21
90	67	0	73	24
120	39	0	55	22

2.2.1.4 PVDF Nanocomposites

The incorporation of metal/inorganic nanoparticles into a polymer matrix has attracted a great deal of interests in the research and industrial fields because the composites with tailored properties desired for particular application or to cover up the drawbacks of the physical properties of polymer can be created (Chae *et al.*, 2007). According to the topic of β-phase induction, there is another method that is addition of external nucleating agents or combination of polymer with nanomaterials. Wang *et al.*, (2011) suggested that polymer nanocomposites had recently been an interesting way to promote β-phase crystal within the polymer and therefore enhance its ferroelectricity. Incorporation of nano-scale materials into a polymer matrix has a greatly improvement on the electrical, thermal and mechanical properties of polymer. Li *et al.*, (2013) indicated that the external nucleating agents afforded available opportunities for gaining high dielectric constant at low filler concentration, allowing polymer nanocomposites to retain their flexibility and mechanical properties. The external nucleating agents such as carbon nanotubes (Ferreira *et al.*, 2012), organoclay (Zhang *et al.*, 2012) and metal nanoparticles (Goncalves *et al.*, 2012).

For carbon fillers, Achaby *et al.*, (2012) statedthat could only induce β-phase formation in PVDF nanocomposites after special modifications of the filler's surface to improve their capability to adsorb PVDF chains. Incorporating a

carbonyl group (-C=O) on the surface of carbon nanotube, resulting in their homogeneous dispersion/distribution because of the strong and specific interaction between the fluorine group (>CF_2) of PVDF and the carbonyl groups (-C=O). The obtained effects were enhancements of the electrical, thermal and mechanical properties of nanocomposites.

For organoclay, Zhang *et al.*, (2012) explained the mechanism for the β-phase formation by adding montmorillonite (MMT) in PVDF. The mechanism was shown in Figure 2.21.

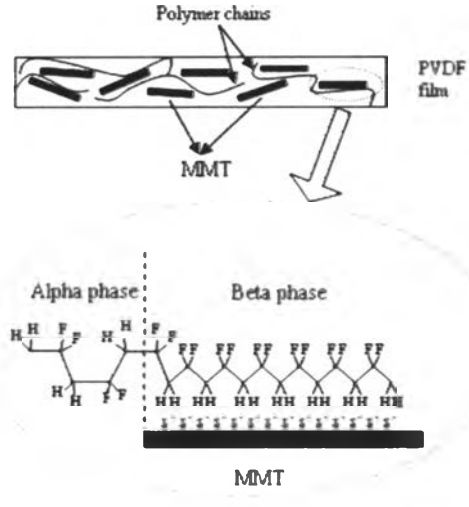

Figure 2.21 Schematic showing the proposed mechanism about β-phase formation (Zhang *et al.*, 2012).

When MMT is added, the MMT acted as substrate of PVDF nucleation. The TTTT conformation chains would be bound on the surface of silicate layers and form β-phase.

For metal-polymer nanocomposites, the crystallization of β-phase was attributed to electrostatic interactions or dipole interaction of the polymer chains with the nanoparticles. This interaction should straighten the PVDF backbone, leading to the formation of TTTT conformation (β-phase) instead of TG^+TG^- conformation (α-phase)

From the experiment by Wang *et al.*, (2011), they believed that the polymorph could be changed by the dipole interaction between the CF dipoles in the PVDF chain and the surface charge on the Au-NP. This could be proved by using FT-IR and DSC technique as shown in Figure 2.22 and 2.23. They observed that PVDF with higher amount of β-phase would have a higher melting point than the α-phase due to the better packing of the TTTT conformation of β-phase PVDF.

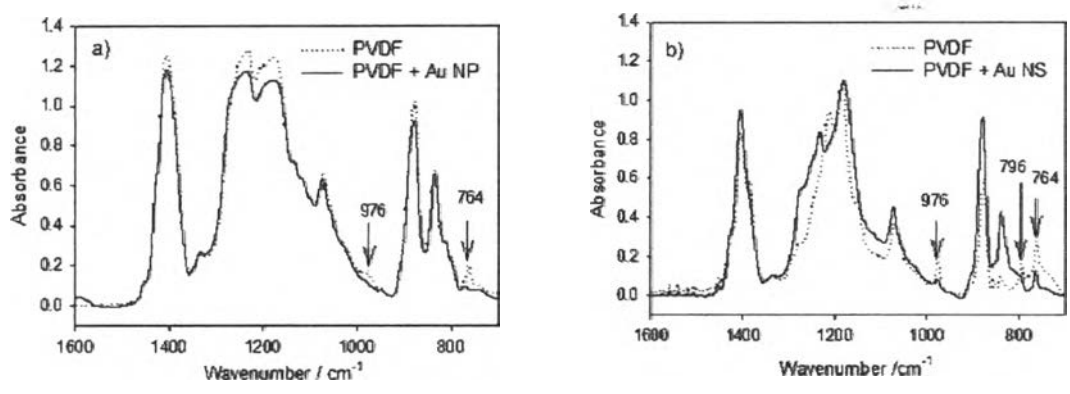

Figure 2.22 FT-IR spectra from dried polymer films of (a) PVDF and Au-NP/PVDF composite, and (b) PVDF and Au-NS/PVDF composite, prepared from mixed solvents of DMF and water. The mass ratio of gold over PVDF in the mixture is 0.5% (Wang *et al.*, 2011).

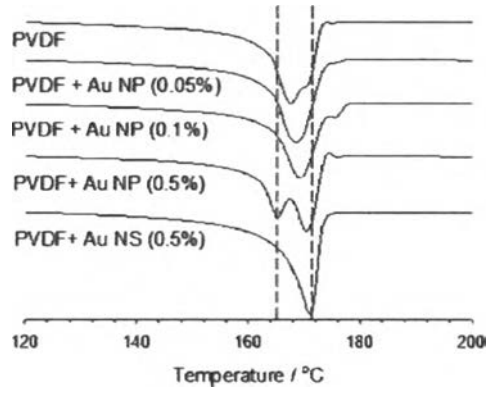

Figure 2.23 DSC melting endotherms of PVDF, Au-NP/PVDF composites with varied gold-to-PVDF mass ratios of 0.5, 0.1 and 0.01% and Au-NS/PVDF composites with gold-to-PVDF mass ratio of 0.5% (Wang *et al.*, (2011).

There's also found the same trend in experiment by Goncalves *et al.*, (2012), they added Fe_2O_3 nanoparticles and the dielectric properties would be investigated. In the Figure 2.24, they found that the increasing of dielectric constant when adding Fe_2O_3 nanoparticles, the explanation was magnetic nanoparticles had the ability to nucleate the electroactive β-phase of the PVDF through surface interactions during the crystallization process of the PVDF phase, resulted the higher β-phase formation. In addition, the dielectric loss is slightly decreased due to decrease ionic mobility of the PVDF due to the interfacial interactions with nanoparticles.

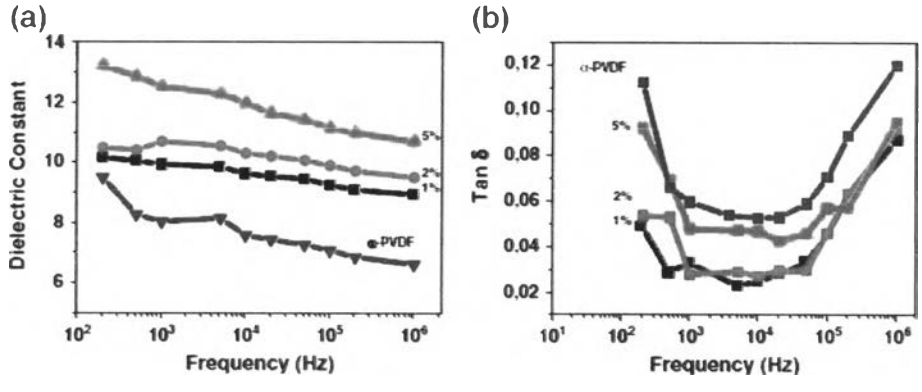

Figure 2.24 Real part of the dielectric constant (a) and dielectric loss (b) obtained for the different IOMNP contents on nanocomposite films as a function of frequency (Goncalves *et al.*, 2012).

In conclusion, the nanoparticles were added to induce the β-phase that's the origin of piezoelectric and dielectric properties in PVDF. The β-phase induction mechanism was occurred by the electrostatic interaction or dipole interaction between surface charge of nanoparticles and the dipole CF_2 on the main chain of PVDF. The highly amount of β-phase.

2.3 Cellulose

The use of cellulose fibers as reinforcing components in polymeric composite materials has been extensively explored during the last decade, mainly in response to the economic and environmental concerns associated with the extensive exploitation of petroleum-derived products. The advantages of cellulose fibers compared with synthetic or inorganic fibers are their biodegradability, renewability, low cost, good thermal-mechanical properties and environmental-friendly. The applications from cellulose-based have been widely used (Trovatti *et al.*, 2010).

In last few years, the incorporation of micro and nano-cellulose fibers, obtained by mechanical, enzymatic or chemical treatments, into several matrices allowed obtaining materials with superior thermal and mechanical properties and transparency (George *et al.*, 2007; Fernandes *et al.*, 2009).

2.3.1 Plant-based Cellulose

A single fiber of all plant-based natural fiber consists of several cells. These cells are formed out of cellulose-based crystalline microfibrils, which are connected to a complete layer by amorphous lignin and hemicelluloses. Multiples of such cellulose-lignin-hemicelluloses layer in one primary and three secondary cell walls stick together to form a multiple layer composite. The fiber strength increases with increasing cellulose content and decreasing spiral angle with respect to fiber axis.

Cellulose is found not to be uniformly crystalline. However, the ordered regions are extensively distributed throughout the material, and these regions are called crystalline. The threadlike entity, which arises from the linear association of these components, is called microfibrils. Its form the basic structural unit of the plant cell wall. Theses microfibrils are found to be 10-30 nm wide, less than this in width, definitely long containing 2-30,000 cellulose molecules in cross section. Their structure consists of predominantly crystalline cellulose core. Individual cellulose nanocrystals (Figure 2.25) are produced by breaking down the cellulose fibers and isolating the crystalline regions (Oke, 2010). These are covered with a sheath of

paracrystalline polyglucosan material surrounded by hemicelluloses (Whistler and Richards, 1970).

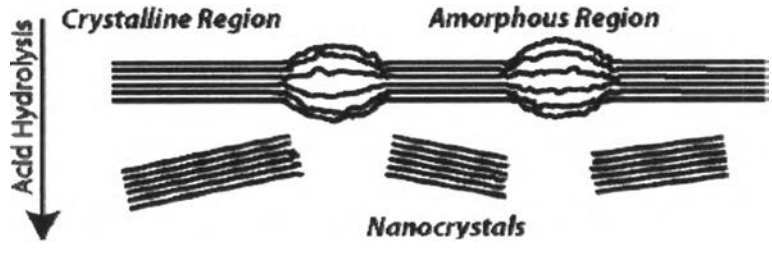

Figure 2.25 Acid hydrolysis breaks down disordered (amorphous) regions and isolates nanocrystals (Oka *et al.*, 2010).

2.3.2 Bacterial Cellulose

Bacterial Cellulose, produced by *Acetobacterxylinum* from Nata de coco when fermented in coconut water (Puspitasari *et al.*, 2006). Nata de coco was chemically treated with alkaline to remove bacterial cell debris (proteins) out of the bacterial cellulose (George *et al.*, 2007; Nogi *et al.*, 2008). This nano-size cellulose was markedly different from cellulose obtained from trees and cotton. From the culture medium a pure cellulose network free of lignin and hemicellulose is obtained as a highly hydrated pellicle made up of a random assembly of ribbon shaped fibers less than 100 nm wide (Barud *et al.*, 2007). These fibers themselves are composed of a bundle of much finer microfibrils of nanometric structure (Ummartyotin *et al.*, 2012). Bacterial cellulose possessed properties that provide, such as high mechanical strength, high crystallinity and a highly pure nanofibrillar network structure, so it's becoming a promising biopolymer for several applications (Barud *et al.*, 2007; Brown *et al.*, 2007).

Fernandes *et al.*, (2009) investigated the effect of bacterial cellulose in chitosan nanocomposite, they found that bacterial cellulose would have intermolecular interaction between hydrogen from hydroxyl group at 6-C on the bacterial cellulose surface with amino group from chitosan, resulted slightly increase the degradation temperature, moreover largely increasing in Young's modulus and tensile

strength even decreasing in strain properties, would be observed. The similar effects also found in the experiment from Brown *et al.*, (2007) and Trovatti *et al.*, (2010) that added bacterial cellulose with polar polymeric material.

More recently, interest of using bacterial cellulosefor transparent electronics device will be higher. Due to their thermal expansion coefficient is low as 0.1 ppm/K, so it could be used as reinforcing in polymer composite material to reduce the thermal expansion coefficient of the polymeric material that was destructed by the temperature fluctuation in transparent electronics device assembly and mounting process because typical polymeric material had very high thermal expansion coefficient (Nogi *et al.*, 2008; Ummartyotin *et al.*, 2012).